Tuning of Ionic Liquid Crystal Properties by Combining Halogen Bonding and Fluorous Effect

Gabriella Cavallo,*[a] Antonio Abate,[b] Marta Rosati,[a] Giovanni Paolo Venuti,[a] Tullio Pilati,[a] Giancarlo Terraneo,[a] Giuseppe Resnati,[a] and Pierangelo Metrangolo[a]

We report halogen-bonded complexes between 1-polyfluoroalkyl-3-alkylimidazolium iodides and mono-iodoperfluoroalkanes of different chain lengths or di-iodoperfluorooctane. ^{19}F NMR analyses revealed that the preferred stoichiometry between the donors and acceptors is 1:1 in the cases of the mono-iodoperfluoroalkanes, and 2:1 with di-iodoperfluorooctane, as a result of the monodentate behavior of the iodide anion (halogen bond acceptor). Single crystal X-ray diffraction analyses showed the presence of a perfluorinated superanion, which interdigitates with the cation fluorinated chains, favoring the formation of lamellar structures. All of the obtained supramolecular complexes exhibit enantiotropic liquid crystalline phases over a broad range of temperatures. Most of the obtained complexes show melting points lower than 100 °C, two of them being liquid at room temperature, thus representing a new family of fluorinated ionic liquid crystals.

Introduction

First established as an eco-friendly alternative to volatile organic solvents, room-temperature ionic liquids (RTILs) have attracted considerable scientific interest over the past years and nowadays find applications in various high-end fields.[1] This interest is due to their unique and useful properties, such as negligible vapor pressure, thermal stability, high ionic conductivity, and a large electrochemical window,[2] which make them ideal electrolytes in various iono-optic and electrochemical devices.[3] Physico-chemical properties of ILs may easily be tuned through a careful choice of the organic cation and its counterion. In particular, it has been reported that introducing specific pendants on several cations induces the formation of mesophases, thus generating ionic liquid-crystalline (ILC) materials.[4] For example, an alkyl chain as long as 12 carbon atoms on one of the imidazolium (Im) nitrogens, e.g., 1-dodecyl-3-methylimidazolium iodide, induces the emergence of a smectic A mesophase.[5] Due to the unique properties of the fluorine atom, fluorination has been exploited to control properties and self-assembly behaviour of ILs.[6] Fluorinated moieties have either been introduced on the anion or the organic cation. Fluorinated ILs display a higher oxygen solubility and lower surface energy if compared to their non-fluorinated analogues and have found applications, among others, in (electro)catalysis and energy storage technologies.[7] Moreover, functionalizing mesogens with perfluorocarbon chains allows to control their mesomorphic behaviour thanks to the *fluorous effect*[8] that promotes the segregation between hydrocarbon and perfluorocarbon chains. It has been reported, in fact, that, for some nonmesomorphic 1-alkyl-3-methylimidazolium iodides, substituting one of the alkyl chains with a partially fluorinated one, induces the emergence of smectic mesophases allowing for a new class of ILCs suitable for applications as quasi-solid electrolytes in dye-sensitized solar cells.[9]

Supramolecular fluorinated liquid crystals (LCs) self-assembled through halogen bond (XB) – the noncovalent interaction involving halogen atoms as electrophilic sites[10] – have also been reported.[11] The high specificity of XB for haloperfluorocarbons represents an easy route to introduce fluorinated moieties into supramolecular materials,[12] while its high directionality has proven to be a powerful tool in the construction of new thermotropic calamitic mesogens starting from nonmesomorphic building blocks.[11] The modularity of this approach allowed to easily introduce new functionalities in the final supramolecular systems.[13] For example, the incorporation of an azo-group into XB-donor molecules afforded supramolecular LC complexes with unique light-responsive properties,[14] while complexation of a ditopic XB-donor with alkoxystilbazole derivatives bearing a terminal methacrylate group in the lateral chain, afforded trimeric mesogens suitable for incorporation into LC elastomeric actuators.[15] LC polymers have also been prepared upon complexation of ditopic XB-donor and acceptor molecules,.[16] At the same time, the self-assembly of the amine hydrochloride derivative of a 4-arm polyethylene glycol with iodoperfluoroalkanes afforded supramolecular mesogens characterized by a highly ordered lamellar structure self-organized up to millimetre scale.[17] More

[a] Prof. Dr. G. Cavallo, Dr. M. Rosati, G. Paolo Venuti, Dr. T. Pilati,
Prof. Dr. G. Terraneo, Prof. Dr. G. Resnati, Prof. Dr. P. Metrangolo
Department of Chemistry, Materials
and Chemical Engineering "Giulio Natta"
Politecnico di Milano
Via L. Mancinelli 7, 20131 Milano (Italy)
E-mail: gabriella.cavallo@polimi.it
[b] Dr. A. Abate
Helmholtz-Zentrum Berlin für Materialien und Energie
Kekuléstraße 5, 12489 Berlin (Germany)

ChemPlusChem

Full Papers
doi.org/10.1002/cplu.202100046

**Chemistry
Europe**
European Chemical
Societies Publishing

recently, we have also reported that nonmesomorphic ionic liquids, *i.e.*, 1-alkyl-3-methylimidazolium iodides, self-assemble with iodoperfluorocarbons[18] or fluorinated azobenzene derivatives[19] driven by the XB and result in a new class of superfluorinated supramolecular ILCs, where mesomorphicity was encoded in the trimeric halogen-bonded superanions. Some of these ILCs, showing smectic mesophases down to RT, may become suitable for the development of RT ionic conductors.

With the hypothesis in mind of exploiting the synergistic combination of XB and fluorous effect to drive mesogen self-assembly and tune transition temperatures, we pursued supramolecular complexes between 1-polyfluoroalkyl-3-alkyl-imidazolium iodides **1** and **2**m, and long-chain iodoperfluor-oalkanes **3**p and **4** (Scheme 1). Our objective was to induce lamellar order by segregation of perfluorinated chains. Even starting from nonmesomorphic self-assembling modules, we obtained smectic mesophases whose temperature transitions were tuned to yield ILCs with large mesophase stability windows below 100 °C. Herein, we describe in detail their syntheses, single-crystal X-ray structures, and mesomorphic behaviours.

Results and Discussion

Materials design

The materials under investigation were obtained by mixing 1-polyfluoroalkyl-3-alkylimidazolium iodides **1** and **2**-m with iodoperfluoroalkanes of different chain lengths (**3**p) or 1,8-diiodoperfluorooctane (**4**), as reported in Scheme 1. Notably, the starting Im salts **1** and **2**-1 show enantiotropic smectic A mesophases, while **2**-3 and **2**-5 are nonmesomorphic in nature, suggesting that the flexibility of propyl and pentyl chains may impact liquid crystallinity. We reasoned that by halogen bonding a long-chain iodoperfluoroalkane to the I− ion of the ILs **2**-3 and **2**-5 could result in a more efficient segregation of the hydrocarbon segments of the molecules and a more compact fluorous layer, thus resulting in a lamellar organization and likely promoting the emergence of a mesophase.
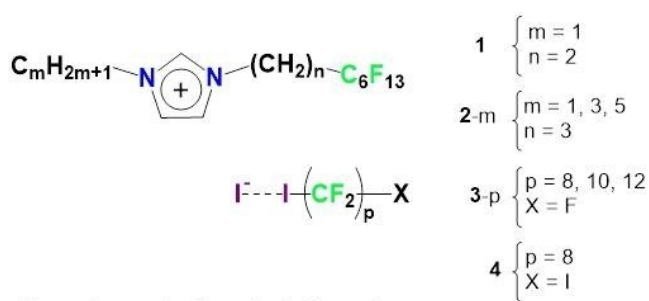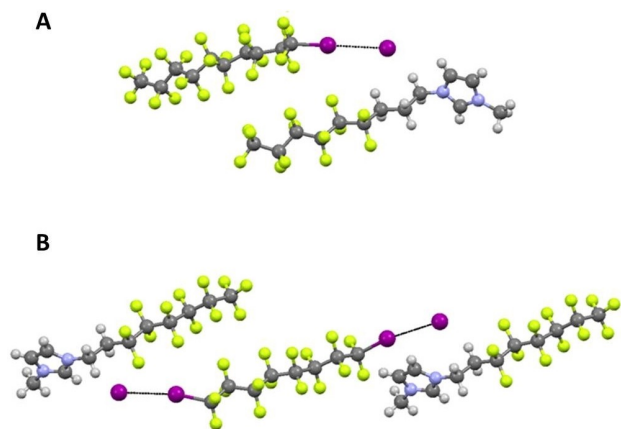
As far as the mixing stoichiometry of starting modules is concerned, it remains challenging to anticipate the composition and structure of the final supramolecular adducts since it is well known that halide anions may function as mono- or poly-dentate XB-acceptors.[20] In particular, the number of XBs that I− ions usually form, depends on the geometry of the interacting moieties, the accessibility of the XB-donor moiety, and the overall requirements of the crystal packing. Therefore, it is quite common to have I− ions functioning as monodentate, bidentate or tridentate XB-acceptors, although higher coordination numbers are also possible.[20] Our previous studies on halogen-bonded superfluorinated ILCs[18,19] would suggest a bidentate behaviour of the I− ion. However, a monodentate behavior action cannot be excluded *a priori*, due to the higher sterical hindrance produced by a fluorinated chain covalently bonded to the Im scaffold.

In order to establish the correct stoichiometric ratio between the Im salt and the iodoperfluoroalkane, we prepared the XB-complexes by isothermal crystallization at RT starting from chloroform solutions containing the XB-donor and accept-or, in either 1:1 or 2:1 ratios. All of the complexes were obtained as white microcrystalline solids that have been fully characterized by ^{1}H and ^{19}F-NMR, DSC, and POM analyses. Good-quality single crystals were also grown for several complexes and submitted to X-ray diffraction analyses.

Single-crystal X-ray structural analyses

Single-crystal X-ray diffraction (XRD) analyses of samples **1·3**-8, **1·3**-10, **1·4**, **2**-1**·3**-10, and **2**-1**·4** revealed common patterns of noncovalent interactions, highlighting how the XB drives the self-assembly between the starting modules. Notably, in all of the cocrystals, the I− ion functions as monodentate XB-acceptor towards the I atoms of the perfluorinated modules. The XB-donor/acceptor ratio in the systems thus depends exclusively on the topicity of the XB-donor. In fact, in complexes **1·3**-8, **1·3**-10, and **2**-1**·3**-10 where the XB-donors are monoiodinated, the XB-donor/acceptor ratio is 1:1 and dimeric halogen-bonded complexes are, thus, formed (Figure 1, top). Similarly, in the complexes **1·4** and **2**-1**·4**, where the XB-donor is diiodoper-fluorooctane **4**, which functions as a ditopic XB-donor, the **1**/**4** and **2**-1/**4** ratios are 2:1 and trimeric complexes are obtained (Figure 1, bottom).

In all of the structures obtained, the C−I···I− contacts, *i.e.*, XBs, are linear (C−I···I− angles between 170.2 and 177.5°) and relatively short (Table 1), confirming the existence of strong and directional interactions.[10] All the C−I···I− distances are quite similar, ranging between 3.434 and 3.503 Å, which corresponds to a *ca.* 13 % reduction of the sum of the van der Waals and Pauling radii for I and I−, respectively, and perfectly in line with those reported in the literature for analogous XB-complexes involving I− ions.[18,19] Interestingly, in all of the analyzed complexes, the I− ions complete their "interaction sphere" forming weak hydrogen bonds (HBs) with the H atom in position 2 of the Im cation, as a consequence of the strong electron-withdrawing effect of the positively charged ring,

Scheme 1. Chemical structures of the used polyfluorinated imidazolium salts (**1** and **2**-m) and iodoperfluoroalkanes (**3**p and **4**), and their halogen-bonded complexes **1·3**p, **1·4**, **2**m**·3**p, and **2**m**·4**.

ChemPlusChem

Full Papers
doi.org/10.1002/cplu.202100046

Chemistry Europe
European Chemical
Societies Publishing

A

B

Figure 1. Top: The asymmetric unit of the complex **2**-1·**3**-10. Halogen bonding drives the self-assembly of the imidazolium salt **2**-1 and the iodoperfluorodecane **3**-10 into a dimeric supramolecular complex. Bottom: The asymmetric unit of the complex **1**·**4**. Halogen bonding drives the self-assembly of the imidazolium salt **1** and diiodoperfluorooctane **4** into a trimeric supramolecular complex. Color code: gray = carbon, blue = nitrogen; magenta = iodine; green = fluorine; light gray = hydrogen. Black dotted lines indicate the halogen bonds.
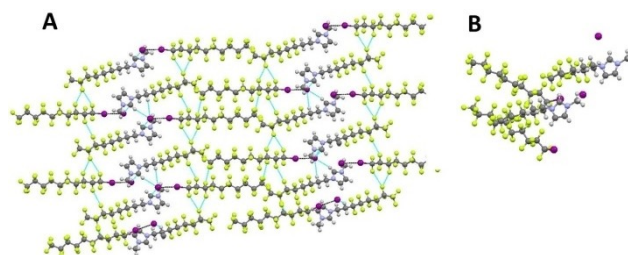
A

B

Figure 2. A) Packing of **2**-1·**3**-10 viewed along the crystallographic *b* axis, showing the segregation between the imidazolium ring and the iodoperfluorooctane module, resulting in a lamellar organization; B) Interdigitation of fluorinated chains from the cation and the halogen-bonded superanion. Color code: gray, carbon; blue, nitrogen; magenta, iodine; green, fluorine; light gray, hydrogen. Black lines indicate the halogen bonds; light blue lines indicate other short contacts.

Table 1. Geometrical features of XB in crystallized complexes.

Complex	$d_{I\cdots I^-}$ [Å]	N_c[a]	C—I···I⁻ Angle [°]
1·**3**-8	3.502	0.87	174.5
1·**3**-10	3.434	0.85	174.0
1·**4**	3.468	0.85	170.2
2–1·**3**-10	3.503	0.87	177.5
2–1·**4**	3.527	0.87	172.8

(a) Nc: Normalized contacts, expressed as the ratio between the XB distance over the sum of the vdW and Pauling radii of the atoms involved in the interaction.

which increases the Lewis-acid character of this H atom. The average H···I⁻ distance in the complexes is ~3 Å, which is in line with those reported in the literature for similar systems.[12] Other weak HBs involving the I⁻ ions are with the methyl group of a nearby ring in cocrystals **1**·**3**-8, **1**·**3**-10, and **1**·**4**.

As far as the crystal packing is concerned, a lamellar organization is observed in all of the complexes elicited by the segregation between the perfluoroalkyl chains and the charged moieties (Figure 2A and Figure S1). The positively charged rings and the iodide anions form a well-defined hydrocarbon layer where each I⁻ unit is surrounded by four imidazolium rings. Specifically, the iodide anion is placed at the center of a supramolecular cube formed by the imidazole rings and shows several short contacts with the electron deficient aromatic area of two imidazolium units (average distance I⁻···centroid of the Im cation: 3.8 Å) and several hydrogen bonding contacts with the H atom in position 2 and the CH₂ units of two other Im cations. The hydrocarbon layers are then surrounded by the fluorinated layers composed by the perfluorinated halogen bonding donor units and the perfluorinated part of the imidazolium moieties. Notably an extended network of F···F contacts (Figure 2A) is present in the fluorinated layers promoting the formation of dense and robust fluorinated lamellar

systems. The resulting lamellar organization, if preserved in the molten state, would most likely determine an LC behaviour with smectic mesophases, as planned in our design. The content of fluorine atoms in these complexes is exceptionally high, picking up to over 53% in **1**·**3**-10. Therefore it was no surprise that perfluoroalkyl chains showed an extensive disorder (Figures S2–S4). This behaviour is quite common in highly-fluorinated crystalline systems and is mainly due to the low ability of fluorine atoms to engage with strong intermolecular interactions, commonly resulting in poorly crystalline materials. Although for some of the reported structures the disorder of the fluorinated chains was quite severe, we were able to locate all the fluorine atoms (see SI for details in the refinement process of the disordered perfluorinated alkyl chains).

NMR analyses

¹⁹F-NMR Spectroscopy was used to determine whether the bulk crystalline samples had the same composition of the analyzed single crystals, *i.e.*, determine the stoichiometric ratio between the Im salt and the iodoperfluoroalkane in all of the complexes under study.

¹⁹F-NMR spectra clearly showed the presence of the characteristic peaks for the two starting fluorinated modules (Figures S5 and S6). In particular, iodoperfluoroalkanes **3**p showed a triplet at −59.86 ppm and a multiplet at −113.12 ppm, due, respectively, to the α and β difluoromethylene groups (I⁻CF_2CF_2−); similarly the diiodoperfluoroocatne **4** showed a triplet at −59.34 ppm (I CF_2−) and a multiplet at 113.08 ppm (I–CF_2CF_2). The Im salts on the contrary showed a multiplet at −113.58 ppm due to the −CH_2CF_2− group. The ratios between the −CH_2CF_2− signal area (derived from the Im) and the (I-CF_2CF_2-) signal areas (derived from the iodoperfluoroalkane) were 1:1 in all of the crystallized complexes, independent of the starting stoichiometry between XB-donor and XB-acceptor modules used in the experiments. This result is perfectly in line with X-ray data. It confirms that the I⁻ functions as monodentate XB-acceptor in all of the bulk complexes and the Im/perfluoroalkane ratios (1:1 for complexes containing **3**p

ChemPlusChem

Full Papers
doi.org/10.1002/cplu.202100046

**Chemistry
Europe**
European Chemical
Societies Publishing

and 1:2 for complexes containing **4**) found in single crystals are representative of the whole bulk samples.

Thermal analyses

The LC properties of the starting Im salts and of all the obtained complexes were established by a combination of Polarised-light Optical Microscopy (POM) and Differential Scanning Calorimetry (DSC) performed on the powder crystalline samples.

Starting Im salts displayed decreasing melting temperatures with increasing hydrocarbon chain lengths. Indeed, while Im salts **1** and **2**-1 have melting points (mp.s) slightly below 100 °C, both **2**-3 and **2**-5 are highly viscous liquids at room temperature (mp.s of −8 and −32 °C, respectively). Furthermore, both **1** and **2**-1 also showed SmA LC properties with clearing points ≥ 200 °C.

Noteworthy, all the obtained complexes showed thermotropic LC properties. Transition temperatures are reported in Table 2. All of the complexes displayed enantiotropic mesomorphism with smectic A phases displaying characteristic optical textures on cooling (Figures 3 and S7). This result is consistent with XRD analyses and is a manifestation of the lamellar organization of perfluorocarbon and hydrocarbon modules. Notably, **2**-3·**3**p and **2**-5·**3**p, although starting Im salts were not LC, all showed the emergence of mesophases. In particular, all of the complexes containing **2**-3 and **2**-5 showed mp.s lower than 80 °C and, noteworthy, **2**-3·**3**-8 and **2**-5·**3**-8 were LC at RT. This result is relevant because RT-LC materials displaying high ionic conductivity are attractive candidates for applications in several electrochemical devices. All of **2**-3·**3**p and **2**-5·**3**p complexes showed clearing points, *i.e.*, SmA-Iso transitions temperatures at ≤ 100 °C and increasing with the length of the halogen-bonded perfluoroalkyl chains. The mesomorphism of **2**-3·**3**p complexes also showed on cooling an intermediate phase, identified by microscopy through the appearance of striations across the back of the fans (Figure 3E), which disappeared on cooling further below the transition. POM texture would suggest the formation of a SmB phase, however other smectic phases or crystal modifications cannot be excluded. Complexes **1**·**3**p all showed melting (≥ 100 °C) and clearing points (≥ 200 °C) higher than the pure **1**, and, in general, provided with the highest transition temperatures and the broadest LC ranges of the whole series of obtained complexes (Figure 4). Conversely, the complex **1**·**4** showed a lower transition temperature. On the other hand, **2**-1·**3**p complexes showed higher melting points while lower clearing points than the pure Im salt **2**-1. In both cases, no particular trends related to the chain length of the perfluorinated

Table 2. Phase transition temperatures and mesophase temperature ranges measured on heating the halogen-bonded complexes **1**·**3**p, **1**·**4**, and **2**m·**3**p.

Complex	Transition[a]	Temperature [°C]	ΔT [°C]
1	Cr–SmA	94	130
	SmA–Iso	224	
1·**3**-8	Cr–SmA	107	127
	SmA–Iso	234	
1·**3**-10	Cr–SmA	99	134
	SmA–Iso	233	
1·**3**-12	Cr–SmA	116	111
	SmA–Iso	227	
1·**4**	Cr–SmA	86	75
	SmA–Iso	161	
2-1	Cr–SmA	86	112
	SmA–Iso	198	
2-1·**3**-8	Cr–SmA	90	55
	SmA–Iso	145	
2-1·**3**-10	Cr–SmA	98	37
	SmA–Iso	135	
2-1·**3**-12	Cr–SmA	120	43
	SmA–Iso	163	
2-3	Cr–Iso	−8	
2-3·**3**-8	Cr–SmA	< 23	97
	(SmA–SmB)[b]	108	
	SmA–Iso	120	
2-3·**3**-10	Cr–SmA	73	62
	(SmA–SmB)[b]	122	
	SmA–Iso	135	
2–3·**3**-12	Cr–SmA	78	61
	(SmA–SmB)[b]	105	
	SmA–Iso	139	
2-5	Cr–Iso	−32	
2-5·**3**-8	Cr–SmA	< 19	80
	SmA–Iso	99	
2-5·**3**-10	Cr–SmA	53	65
	SmA–Iso	118	
2-5·**3**-12	Cr–SmA	52	75
	SmA–ISO	127	

[a] Crystal phase (Cr), smectic A phase (SmA), smectic B phase (SmB), and isotropic phase (Iso). [b] Seen only on cooling.
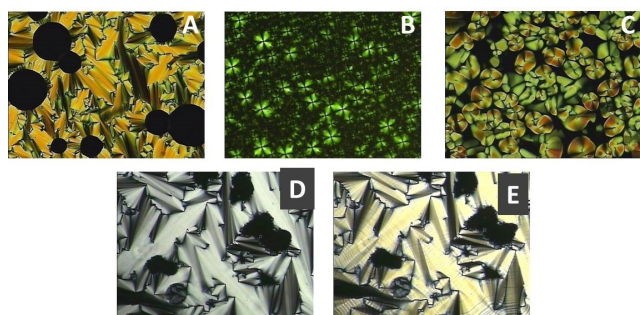
Figure 3. Optical textures observed on cooling from the isotropic state for: A) **1**·**3**-8 at 220 °C; B) **2**-1·**3**-10 at 133 °C; C) **2**-5·**3**-8 at 97 °C; D) **2**-3·**3**-10 at 126 °C (SmA phase); E) **2**-3·**3**-10 at 114 °C (SmB phase).
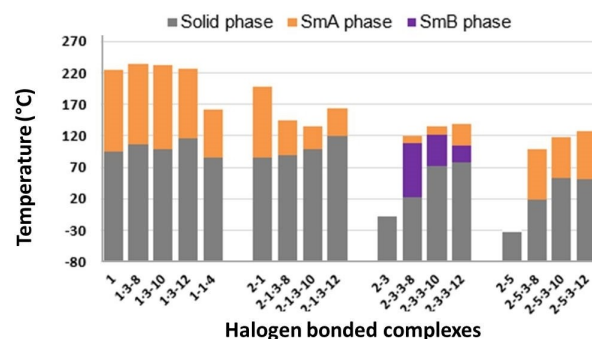
Figure 4. Phase transition temperatures and mesophase temperature ranges measured on heating the halogen-bonded complexes under a hot-stage polarized optical microscope. The smectic B phase has been seen only on cooling for complexes containing **2**-3p.

modules were observed. As far as the length of the alkyl chains on the Im cations, instead, transition temperatures consistently decreased with the increase of the chain length from **1** to **2** m.

Despite the high clearing points, DSC analyses confirmed the stability of such complexes (Figures S8 and S9). Repeated heating and cooling cycles demonstrated that the LC properties were fully reversible over, at least, three cycles, and typical POM features were perfectly reproducible even after several excursions into the isotropic phases. Since **2**-3 and **2**–5 are not mesomorphic, this implies that the XB between the I⁻ ion and the iodoperfluorocarbon survives in the mesophase and is responsible for the LC behaviours of the obtained supramolecular structures. In addition, the formation of halogen bonds also plays a key role in the assembly and stabilization of the observed lamellar arrangements and thus on the formation of the ordered SmA phases. Specifically, the selected XB acceptor modules, composed by an ionic head and a fluorinated tail, are self-assembled amphiphilic systems in nature and their assembly is promoted by strong electrostatic interactions in the layers of the ion pair units (namely the imidazolium ring and the iodide anion) and by multiple F···F contacts for the organization of the fluorinated tails in the fluorinated layers. This amphiphilic character is clearly observed in the XRD studies and it is responsible for the overall lamellar arrangement of the complexes. Here the addition of perfluorinated XB donors has two-folds effect on the overall organization. First there is, for all the complexes, an elongation of the perfluorinated portion which adds a further stabilization of the fluorinated layers thanks to the formation of additional F···F contacts. Latter it is able to induce, for the non-mesomorphic salts **2**-3 and **2**-5, the LC behavior. Therefore the formation of liquid crystalline phases with lamellar order can be affected by a careful selection of the length of perfluorinated chains which can be added using a supramolecular approach driven by XB.

Conclusion

We have described the synthesis of new supramolecular complexes obtained upon XB-driven self-assembly of 1-polyfluoroalkyl-3-alkylimidazolium iodides (**1** and **2** m) and mono-iodoperfluoroalkanes of different chain lengths (**3** p) or diiodoperfluorooctane (**4**). Single crystal X-ray diffraction analyses proved that I···I⁻ halogen bonds are primarily responsible for the self-assembly of the complementary modules, driving the formation of perfluorinated superanions. The partial interdigitation of fluorinated chains of anions and cations interacting through weak F···F contacts enhances the segregation between perfluorocarbon and hydrocarbon moieties promoting the formation of the segregated layered structure.

All of the complexes displayed thermotropic liquid-crystalline behaviour over a wide range of temperatures, with enantiotropic smectic phases, which are reminiscent of the lamellar phase observed in the crystal state. Notably, some complexes are liquid crystalline at room temperature providing new fluorinated ionic liquid crystalline materials. Our results highlight the ability of the XB to persist in the molten/liquid phase and work as an efficient supramolecular tool for the introduction of long perfluoroalkyl chains on the anions of imidazolium salts, thus providing novel design principles for supramolecular ionic conductors.

Experimental Section

Materials and Methods

The starting materials were purchased from Sigma-Aldrich, Acros Organics, and Apollo Scientific and they were used as received. Commercial HPLC-grade solvents were used without further purification. The LC textures were studied with an Olympus BX51 polarized optical microscope equipped with a Linkam Scientific LTS 350 heating stage and a Sony CCD-IRIS/RGB video camera. DSC analysis was performed with a Mettler Toledo DSC823e instrument, using aluminum light 20 μL sample pans and Mettler STARe software for calculation. ¹H NMR and ¹⁹F NMR spectra were recorded at 25 °C with a Bruker AV 500 spectrometer using CDCl₃ as a solvent. TMS and CFCl₃ were used as internal standards for calibrating chemical shifts in ¹H NMR and ¹⁹F NMR, respectively. The single-crystal X-ray structures were determined on a Bruker Kappa Apex II diffractometer. Experimental details about the crystal structure determination can be found in the Supporting Information

Synthesis

All the 1-polyfluoroalkyl-3-alkylimidazolium iodides (**1** and **2**-m) were prepared as previously reported.[7] The supramolecular complexes were synthesized as follows: The 1-polyfluoroalkyl-3-alkyl imidazolium iodides and the appropriate iodoperfluoroalkanes were dissolved separately in chloroform. The two solutions were mixed in an open, clear borosilicate glass vial to obtain a 1:1 or a 1:2 imidazolium/perfluorocarbon molar ratio. The slow evaporation of the solvent at room temperature afforded to microcrystalline powders which have been characterized by ¹H and ¹⁹F NMR.

Single crystal X-ray diffraction analysis

Single crystals suitable for X-Ray diffraction analysis were obtained through free-interface diffusion crystallization experiments carried out at the interface between chloroform and hexane. In this case, the imidazolium salts were dissolved in chloroform, while perfluorocarbons were dissolved in hexane. The hexane solution was then stratified on the chloroform solution and the slow diffusion of the hexane in chloroform afforded to good quality single crystals. Deposition Numbers 784681 (for **1**·**3**-8), 784679 (for **1**·**3**-10), 784677 (for **1**·**4**), 784680 (for **2**-1·**3**-10) and 784678 (for **2**·**4**) contain the supplementary crystallographic data for this paper. These data are provided free of charge by the joint Cambridge Crystallographic Data Centre and Fachinformationszentrum Karlsruhe Access Structures service www.ccdc.cam.ac.uk/structures.

Conflict of Interest

The authors declare no conflict of interest.

Keywords: fluorous effects · halogen bonding · ionic liquids · liquid crystals · self-assembly

[1] a) M. Smiglak, J. M. Pringle, X. Lu, L. Han, S. Zhang, H. Gao, D. R. MacFarlane, R. D. Rogers, *Chem. Commun.* **2014**, *50*, 9228–9250; b) N. V. Plechkova, K. R. Seddon, *Chem. Soc. Rev.* **2008**, *37*, 123–150; c) G. G. Eshetu, M. Armand, B. Scrosati, S. Passerini, *Angew. Chem. Int. Ed.* **2014**, *53*, 13342–13359; *Angew. Chem.* **2014**, *126*, 13558–13576; d) R. Giernoth, *Angew. Chem. Int. Ed.* **2010**, *49*, 2834–2839; *Angew. Chem.* **2010**, *122*, 2896–2901; e) A.-L. Kubo, L. Kremer, S. Herrmann, S. G. Mitchell, O. M. Bondarenko, A. Kahru, C. Streb, *ChemPlusChem* **2017**, *82*, 867–871; f) Ł. Klapiszewski, T. J. Szalaty, B. Kurc, M. Stanisz, B. Zawadzki, A. Skrzypczak, T. Jesionowski, *ChemPlusChem* **2018**, *83*, 361–374; g) K. S. Schaffarczyk McHale, R. S. Haines, J. B. Harper, *ChemPlusChem* **2019**, *84*, 465–473; h) Q. Luo, E. Pentzer, *ACS Appl. Mater. Interfaces* **2020**, *12*, 5, 5169–5176; i) P. Chen, L. Zhang, J.-S. Sun, E.-K. Xiao, X.-T. Wu, G. Zhu, *ChemPlusChem* **2020**, *85*, 943–947; j) C. H. Park, V. Schroeder, B. J. Kim, T. M. Swager, *ACS Sens.* **2018**, *3*, 2432–2437.

[2] a) K. R. Seddon, *Nat. Mater.* **2003**, *2*, 363–365; b) I. Jerman, V. Jovanovski, A. Surca Vuk, S. B. Hocevar, M. Gaberscek, A. Jesih, B. Orel, *Electrochim. Acta* **2008**, *53*, 2281–2288; c) C. Simocko, Y. Yang, T. M. Swager, K. B. Wagener, *ACS Macro Lett.* **2013**, *2*, 1061–1064.

[3] a) H. Liu, H. Yu, *J. Mater. Sci. Technol.* **2019**, *35*, 674–686; b) M. Watanabe, M. L. Thomas, S. Zhang, K. Ueno, T. Yasuda, K. Dokko, *Chem. Rev.* **2017**, *117*, 7190–7239; c) Q. Yang, Z. Zhang, X.-G. Sun, Y.-S. Hu, H. Xing, S. Dai, *Chem. Soc. Rev.* **2018**, *47*, 2020–2064. d) A. Turguła, M. Graś, A. Gabryelczyk, G. Lota, J. Pernak, *ChemPlusChem* **2020**, *85*, 2679–2688; e) P. Staeld, M. Kaller, P. Ehni, M. Ebert, S. Laschat, F. Giesselmann, *Crystals* **2019**, *9*, 74–93.f) T. Onuma, E. Hosono, M. Takenouchi, J. Sakuda, S. Kajiyama, M. Yoshio, T. Kato *ACS Omega* **2018**, *3*, 159–166

[4] a) C. J. Bowlas, D. W. Bruce, K. R. Seddon, *Chem. Commun.* **1996**, 1625–1626; b) K. V. Axenov, S. Laschat, *Materials* **2011**, *4*, 206–259; c) K. Binnemans, *Chem. Rev.* **2005**, *105*, 4148–4204; d) C. Tschierske, *Angew. Chem. Int. Ed.* **2013**, *52*, 8828–8878; *Angew. Chem.* **2013**, *125*, 8992–9047; e) R. Forschner, J. Knelles, K. Bader, C. Meller, W. Frey, Y. Molard, F. Giesselmann, S. Laschat, *Chem. Eur. J.* **2019**, *25*, 12966–12980; f) T. Ichikawa, T. Kato, H. Ohno, *Chem. Commun.*, **2019**, *55*, 8205–8214

[5] N. Yamanaka, R. Kawano, W. Kubo, N. Masaki, T. Kitamura, Y. Wada, M. Watanabe, S. Yanagida, *J. Phys. Chem. B* **2007**, *111*, 4763–4769.

[6] a) M. Hird, *Chem. Soc. Rev.* **2007**, *36*, 2070–2095 b) L. M. J. Moore, K. T. Greeson, N. D. Redeker, J. J. Zavala, T. C. Le, L. V. Gilmore, K. B. Thompson, J. C. Marcischak, A. S. Quintana, S. J. Teat, A. J. Guenthner, K. B. Ghiassi *J. Mol. Liq.* **2019**, *295* 111677–111686; c) E. Jean, D. Villemin, L. Lebrun *J. Fluor. Chem.* **2019**, *227* 109365 – 109371; d) M. Hummel, M. Markiewicz, S. Stolte, M. Noisternig, D. E. Braun, T. Gelbrich, U. J. Griesser, G. Partl, B. Naier, K. Wurst, B. Krüger, H. Kopacka, G. Laus, H. Huppertzd, H. Schottenberger, *Green Chem.* **2017**, *19*, 3225–3237.

[7] a) G. Vanhoutte, S. D. Hojniak, F. Bardé, K. Binnemans, J. Fransaer, *RSC Adv.* **2018**, *8*, 4525–4530; b) L. M. J. Moore, K. T. Greeson, N. D. Redeker, J. J. Zavala, T. C. Le, L. V. Gilmore, K. B. Thompson, J. C. Marcischak, A. S. Quintana, S. J. Teat, A. J. Guenthner, K. B. Ghiassi, *J. Mol. Liq.* **2019**, *295*, 111687–111698

[8] a) H. Miyajima, M. C. Z. Kasuya, A. Del Guerzo, J.-M. Vincent, K. Hatanaka, *J. Fluorine Chem.* **2018**, *205*, 30–34; b) J.-M. Vincent, M. Contel, G. Pozzi, R. H. Fish, *Coord. Chem. Rev.* **2019**, *380* 584–599; c) C. Rocaboy, F. Hampel, J. A. Gladysz, *J. Org. Chem.* **2002**, *67*, 6863–6870; d) J. A. Gladysz, M. Jurisch (**2011**) Structural, Physical, and Chemical Properties of Fluorous Compounds. In: Horváth I. (eds) Fluorous Chemistry. Topics in Current Chemistry, vol 308. Springer, Berlin, Heidelberg. https://doi.org/10.1007/128 2011 282

[9] a) A. Abate, A. Petrozza, G. Cavallo, G. Lanzani, F. Matteucci, D. W. Bruce, N. Houbenov, P. Metrangolo, G. Resnati, *J. Mater. Chem. A* **2013**, *1*, 6572–6578; b) A. Abate, A. Petrozza, V. Roiati, S. Guarnera, H. Snaith, F. Matteucci, G. Lanzani, P. Metrangolo, G. Resnati, *Org. Electron.* **2012**, *13*, 2474–2478; c) T. L. Merrigan, E. D. Bates, S. C. Dorman, J. H. Davis Jr, *Chem. Commun.* **2000**, *20*, 2051–2052; d) R. P. Singh, S. Manandhar, J. M. Shreeve, *Tet. Let.* **2002**, *43*, 9497–9499.e) D. Hçgberg, B. Soberats, M. Yoshio, Y. Mizumura, S. Uchida, L. Kloo, H. Segawa, T.i Kato *ChemPlusChem* **2017**, *82*, 834–840

[10] G. R. Desiraju, P. S. Ho, L. Kloo, A. C. Legon, R. Marquardt, P. Metrangolo, P. Politzer, G. Resnati, K. Rissanen, *Pure Appl. Chem.* **2013**, *85*, 1711–1713.

[11] a) D. W. Bruce, W. In Halogen Bonding. Fundamentals and Applications; Vol. 126 Structure and Bonding; (Eds. P. Metrangolo, G. Resnati) Springer-Verlag: Berlin Heidelberg, **2008**, pp 161–180; b) L. J. McAllister, C. Präsang, J. P. Wong, R. J. Thatcher, A. C. Whitwood, B. Donnio, P. O'Brien, P. B. Karadakov, D. W. Bruce, *Chem. Commun. (Camb.)* **2013**, *49*, 3946–3948; c) H. L. Nguyen, P. N. Horton, M. B. Hursthouse, A. C. Legon, D. W. Bruce, *J. Am. Chem. Soc.* **2004**, *126*, 16–17.

[12] a) A. Priimagi, G. Cavallo, P. Metrangolo, G. Resnati, *Acc. Chem. Res.* **2013**, *46*, 2686–2695; b) G. Cavallo, P. Metrangolo, R. Milani, T. Pilati, A. Priimägi, G. Resnati, G. Terraneo, *Chem. Rev.* **2016**, *116*, 2478–2601; c) L. C. Gilday, S. W. Robinson, T. A. Barendt, M. J. Langton, B. R. Mullaney, P. D. Beer, *Chem. Rev.* **2015**, *115*, 7118–7195; d) F. Pan, M. Dashti, M. R. Reynolds, K. Rissanen, J. F. Trant, N. K. Beyeh *Beilstein J. Org. Chem.* **2019**, *15*, 947–954; e) F. Topić, K. Rissanen, *Am. Chem.* **2016**, *138*, 6610–6616

[13] H. Wang, H. Bisoyi, A. Urbas, T. Bunning, Q. Li, *Chem. A Eur. J.* **2019**, *25*, 1369–1378

[14] a) A. Priimagi, M. Saccone, G. Cavallo, A. Shishido, T. Pilati, P. Metrangolo, G. Resnati, *Adv. Mater.* **2012**, *24*, OP345-OP352: b) F. Fernandez-Palacio, M. Poutanen, M. Saccone, A. Siiskonen, G. Terraneo, G. Resnati, O. Ikkala, P. Metrangolo, A. Priimagi, *Chem. Mater.* **2016**, *28*, 8314–8321; c) Y. Chen, H. Yu, L. Zhang, H. Yang, Y. Lu, *Chem. Commun.* **2014**, *50*, 9647–9649.

[15] V. Kumar, D. J. Mulder, G. Cavallo, T. Pilati, G. Terraneo, G. Resnati, A. P. H. J. Schenning, P. Metrangolo, *J. Fluorine Chem.* **2016**, *198*, 54–60.

[16] J. Xu, X. Liu, T. Lin, J. Huang, C. He, *Macromolecules* **2005**, *38*, 3554–3557.

[17] N. Houbenov, R. Milani, M. Poutanen, J. Haataja, V. Dichiarante, J. Sainio, J. Ruokolainen, G. Resnati, P. Metrangolo, O. Ikkala, *Nat. Commun.* **2014**, *5*, 4043–4055.

[18] G. Cavallo, G. Terraneo, A. Monfredini, M. Saccone, A. Priimagi, T. Pilati, G. Resnati, P. Metrangolo, D. W. Bruce, *Angew. Chemie-Int. Ed.* **2016**, *55*, 6300–6304.

[19] M. Saccone, F. Fernandez Palacio, G. Cavallo, V. Dichiarante, M. Virkki, G. Terraneo, A. Priimagi, P. Metrangolo, *Faraday Discuss.* **2017**, *203*, 407–422.

[20] a) T. L. Merrigan, E. D. Bates, S. C. Dorman, J. H. Davis Jr, *Chem. Commun.* **2000**, *20*, 2051–2052; b) R. P. Singh, S. Manandhar, J. M. Shreeve, *Tet. Let.* **2002**, *43*, 9497–9499.

[21] a) A. Brown, P. D. Beer, *Chem. Commun.* **2016**, *52*, 8645–8658; b) G. Cavallo, P. Metrangolo, T. Pilati, G. Resnati, M. Sansotera, G. Terraneo, *Chem. Soc. Rev.* **2010**, *39*, 3772–3783; c) J. Y. C. Lim, P. D. Beer, *Chem* **2018**, *4*, 731–783.

[22] P. Metrangolo, T. Pilati, G. Terraneo, S. Biella, G. Resnati, *CrystEngComm* **2009**, *11*, 1187–1196.